

Geophysical Research Letters[®]

RESEARCH LETTER

10.1029/2025GL116328

Challenges in Determining Whether ENSO Is a Damped or a Self-Sustained Oscillation



Key Points:

- It is still not clear whether ENSO is a damped stochastically-driven oscillation or a self-sustained one
- Fitting the Recharge Oscillator model via multivariate linear regression systematically underestimates the growth rate of ENSO
- It is therefore challenging to diagnose whether the observed ENSO is in a damped or self-sustained regime using this approach

Supporting Information:

Supporting Information may be found in the online version of this article.

Correspondence to:

E. Weeks,
elleweeks@g.harvard.edu

Citation:

Weeks, E., & Tziperman, E. (2025). Challenges in determining whether ENSO is a damped or a self-sustained oscillation. *Geophysical Research Letters*, 52, e2025GL116328. <https://doi.org/10.1029/2025GL116328>

Received 15 APR 2025

Accepted 4 AUG 2025

Elle Weeks¹  and Eli Tziperman^{1,2} 

¹School of Engineering and Applied Sciences, Harvard University, Cambridge, MA, USA, ²Department of Earth and Planetary Sciences, Harvard University, Cambridge, MA, USA

Abstract The recharge oscillator (RO) model has been successfully used to understand different aspects of the El Niño–Southern Oscillation (ENSO). Fitting the RO to observations and climate model simulations consistently suggests that ENSO is a damped oscillator whose variability is sustained and made irregular by external weather noise. We investigate the methods that have been used to estimate the growth rate of ENSO by applying them to simulations of both damped and self-sustained RO regimes. We find that fitting a linear RO leads to parameters that imply a damped oscillator even when the fitted data were produced by a model that is self-sustained. Fitting a nonlinear RO also leads to a significant bias toward the damped regime. As such, it seems challenging to decide whether ENSO is a damped or a self-sustained oscillation by fitting such models to observations, and the possibility that ENSO is self-sustained cannot be ruled out.

Plain Language Summary The El Niño Southern Oscillation (ENSO) is the largest driver of year-to-year global climate variability. An important question still unresolved is whether ENSO is driven by weather variability (noise, random forcing) or is self-sustained and would have existed without such random forcing. Addressing this often involves fitting a conceptual, often linear, model to observations of ENSO or to climate model output to estimate its characteristics such as the period and growth rate. Using this approach, previous studies typically estimate a negative growth rate suggesting that ENSO is a damped system requiring random wind events to sustain it. In this study, we investigate these methods for estimating the ENSO growth rate from observations and find that the growth rate is likely being substantially underestimated by such a fit. Our results imply that it is possible that the true ENSO growth rate could be positive implying that we cannot rule out that the ENSO cycle could exist without the need for external weather forcing.

1. Introduction

The El Niño Southern Oscillation (ENSO) is the dominant mode of interannual variability in the equatorial Pacific. ENSO teleconnections communicate its effects globally, making it a key driver of interannual climate variations (Timmermann et al., 2018). General circulation models (GCMs) reproduce many key features of ENSO but are limited by several biases and are computationally expensive to run (Guilyardi et al., 2020; Latif et al., 2001; Planton et al., 2021). Additionally, future projections are inconsistent in their predictions of ENSO amplitude, period, and pattern across models (Chen et al., 2017; Maher et al., 2023; Vecchi & Wittenberg, 2010). As such, simple conceptual models represent a useful tool for understanding ENSO. Several simple models have been developed and used to advance our understanding of the dynamics of the ENSO system (Neelin et al., 1998), including the delayed oscillator (Battisti & Hirst, 1989; Suarez & Schopf, 1988) and the recharge oscillator (RO) models (Jin, 1997a, 1997b; Vialard et al., 2025). The recharge oscillator, which is the main tool used here, is represented by two ordinary differential equations describing the evolution of the ENSO sea surface temperature (SST) and equatorial heat content anomalies. The processes described by the model include the Bjerknes feedback in which SST anomalies intensify rapidly, the slow equatorial heat content adjustment mediated by Kelvin and Rossby waves, and the delayed oceanic feedback in which cooling occurs due to upwelling and westward currents (Jin, 1997a). Further work extended the RO to include stochastic forcing and nonlinear effects (Battisti & Hirst, 1989; Jin, 1997a; Jin et al., 2007; Perez et al., 2005; Schopf & Suarez, 1988; Vialard et al., 2025).

Previous work has used the RO to study many aspects of ENSO dynamics, including the stability of the system (Burgers et al., 2005; Jin et al., 2006; Kim & Jin, 2011; Kim et al., 2014), the predictability of ENSO (Frauen & Dommenget, 2012; Jin et al., 2007; Levine & McPhaden, 2015), the asymmetry between El Niño and La Niña events (Frauen & Dommenget, 2010), and the diversity of ENSO events (Capotondi et al., 2020; Wengel

© 2025. The Author(s).

This is an open access article under the terms of the [Creative Commons Attribution License](https://creativecommons.org/licenses/by/4.0/), which permits use, distribution and reproduction in any medium, provided the original work is properly cited.

et al., 2018; Yu et al., 2016), among others (Jansen et al., 2009; Vijayeta & Dommenget, 2018). One important application involves fitting the RO to observations or comprehensive climate model output to estimate the RO parameters, which can be used to quantify feedback strengths, the ENSO amplitude, or the stability (Burgers et al., 2005; Frauen & Dommenget, 2012; Jansen et al., 2009; Vialard et al., 2025; Vijayeta & Dommenget, 2018; Wengel et al., 2018). The stability of ENSO is characterized by its growth rate—a negative growth rate implying a stable, damped regime and a positive growth rate implying an unstable, self-sustained regime. In particular, the Bjerknes-Wyrki-Jin (BWJ) index allows one to quantify both the ENSO growth rate and period using the diagnosed RO parameters (Jin et al., 2006, 2020; Lu et al., 2018). In practice, fitting the linear recharge oscillator to observations and climate model output consistently yields a negative growth rate, suggesting that ENSO is a damped oscillator sustained by stochastic forcing (Burgers et al., 2005; Vialard et al., 2025; Wengel et al., 2018). However, as carefully noted by Burgers et al. (2005) and discussed in Jin (1997a), weakly damped and slightly supercritical systems (i.e., positive growth rate near zero) may appear very similar in the presence of noise. Additionally, alternative models of ENSO suggest that the dynamics could instead be described by a self-sustained chaotic regime (Chang et al., 1996; Tziperman et al., 1994, 1995; Vallis, 1986).

In this work, we investigate the accuracy of methods that have been used to estimate the RO parameters and subsequently estimate the growth rate and period of ENSO from observations or climate model output. Using simulations of a nonlinear recharge oscillator in which the true RO parameters are known, we quantify the errors in the parameter estimates and determine if standard methods can distinguish between a damped regime and a self-sustained regime. We find that fitting a linear RO consistently results in parameter estimates that imply a damped system, even when the fitted data were simulated by a self-sustained model. Applying these fitting methods over a range of parameter values shows that the growth rate is frequently underestimated, even when the model used to fit the data exactly matches the model used to generate them. Ultimately, these results point to the challenges in robustly differentiating between a damped or a self-sustained ENSO regime.

2. Data and Methods

The Recharge Oscillator model (Burgers et al., 2005; Jin, 1997a; Vialard et al., 2025) describes the evolution of the eastern equatorial Pacific SST and the equatorial Pacific heat content. In its simplest form, the RO is based on the following two linear ordinary differential equations, referred to as the linear recharge oscillator (LRO),

$$\frac{dT}{dt} = RT + F_1 h + \zeta_T \quad (1)$$

$$\frac{dh}{dt} = -\epsilon h - F_2 T + \zeta_h, \quad (2)$$

where T is the eastern equatorial Pacific SST anomaly, and h is the equatorial Pacific thermocline depth anomaly. The parameter R represents the Bjerknes feedback, the parameter ϵ captures the ocean basin adjustment mediated by Rossby and Kelvin waves, the $-F_2 T$ term represents the effect of the Sverdrup transport on h , and the $F_1 h$ term represents the delayed effects on T through upwelling and westward currents. The stochastic forcing terms ζ_T and ζ_h primarily represent the weather forcings due to wind stress, including by westerly wind bursts that are known to depend on the SST (Harrison & Vecchi, 1997; Jin, 1997a; Jin et al., 2020; Tziperman & Yu, 2007).

The LRO describes a harmonic oscillator whose growth rate, γ , and frequency, ω , are given by the real and complex parts of the Bjerknes–Wyrki–Jin (BWJ) index, respectively (Jin et al., 2006, 2020; Lu et al., 2018).

$$\gamma = \frac{R - \epsilon}{2} \quad (3)$$

$$\omega = \sqrt{F_1 F_2 - \frac{(R + \epsilon)^2}{4}} \quad (4)$$

Inferring a negative growth rate using the BWJ index implies a damped system, while inferring a positive growth rate implies a self-sustained one.

To better capture some of the complexities of the ENSO behavior such as the asymmetry between the El Niño and La Niña states, nonlinearities can be introduced into the RO model. We will refer to the model described by the following set of differential equations as the nonlinear recharge oscillator (NRO),

$$\frac{dT}{dt} = RT + F_1h + bT^2 + cT^3 + \zeta_T \quad (5)$$

$$\frac{dh}{dt} = -\epsilon h - F_2T + \zeta_h. \quad (6)$$

Here, the quadratic nonlinearity (bT^2 , $b > 0$) represents the physical processes that favor the growth of El Niño relative to La Niña leading to larger amplitude and shorter El Niño events (Frauen & Dommenget, 2010). The cubic nonlinearity (cT^3 , $c < 0$) represents saturation effects on the ENSO amplitude (Battisti & Hirst, 1989; Jin, 1997a; Schopf & Suarez, 1988).

In this work, we will explore the parameter values obtained by fitting both the LRO and the NRO equations to observations and simulated data.

For observations, we use the ORAS5 ocean reanalysis product from 1958 to 2020 (Copernicus Climate Change Service, 2021). We use the monthly mean time series for the sea surface temperature (SST) averaged over the Niño3 region (5°N – 5°S , 150°W – 90°W) and the thermocline depth defined as the 20°C isotherm depth averaged over the equatorial Pacific (5°N – 5°S , 120°E – 80°W). We compute monthly anomalies by subtracting the corresponding mean for each month over the full time series.

We generate time series of T and h for which we know the true generative model and parameter values by integrating the RO equations. We perform this integration using a forward Euler method with a time step of 1 day and red noise stochastic forcing terms with a decorrelation timescale of 3 days following Vijayeta and Dommenget (2018) and Wengel et al. (2018). The integrations are performed using the NRO Equations 5 and 6. We simulate time series of daily anomalies and compute monthly averages of the simulated daily data to obtain monthly mean anomalies.

For the analysis shown below, we perform simulations for two cases, a damped oscillatory regime and a self-sustained oscillatory regime. The RO parameters for the damped parameter regime were calculated by fitting the NRO equations to monthly mean anomalies computed from the ORAS5 reanalysis product. They are consistent with previous work estimating the RO parameters from observations (Burgers et al., 2005; Vialard et al., 2025; Vijayeta & Dommenget, 2018; Wengel et al., 2018). This damped oscillator has a decay timescale of 1.7 years and period of 3.7 years. For the self-sustained oscillator regime, we chose RO parameters such that the oscillator had a growth timescale of 11 years and shared features with the damped oscillator, such as the period, spectrum, and shape of the distributions of T and h . The magnitude of the stochastic forcing terms, ζ_T and ζ_h , are the same across all simulations. The RO parameters used in the simulations for these two cases are listed in Table S1 in Supporting Information S1. For both regimes, we simulated 100 time series for a duration of 150 years each and perform our analyses using the last 100 years.

In addition, we simulate another set of 10,000 RO time series in which the values of all NRO parameters (R , ϵ , F_1 , F_2 , b , c , $\text{std}(\zeta_T)$, and $\text{std}(\zeta_H)$) are varied randomly. Again, each time series was simulated for a duration of 150 years, and results are from the last 100 years. For these simulations, we allow all parameters to vary independently of each other. Han et al. (2025) explored the parameter space while fixing $R + \epsilon$ to preserve the period; we chose to allow for growth rates between -1 and 1 years^{-1} , periods between 1 and 10 years, and any combination of these.

Finally, we estimate the RO parameters from observations and simulated time series. We follow previous studies and estimate the RO parameters by fitting the LRO Equations 1 and 2 via multivariate linear regression of monthly mean tendencies of T and h against monthly mean anomalies of T and h from observations or model output (Burgers et al., 2005; Vialard et al., 2025; Vijayeta & Dommenget, 2018; Wengel et al., 2018). Following the above previous studies that fitted the RO to observations and model output, we compute the monthly mean tendencies using a forward difference approximation, for example, $(T_{n+1} - T_n)/\Delta t = RT_n + F_1h_n$, where n indicates monthly values and Δt is 1 month. We perform linear regression of the monthly mean tendencies of T on

monthly mean anomalies of T and h to obtain estimates for parameters R and F_1 . We perform a separate linear regression of the monthly mean tendencies of h on monthly mean anomalies of h and T to obtain estimates for parameters ϵ and F_2 . The standard deviation of the stochastic forcing terms can then be approximated by the standard deviation of the residuals of the linear regression fit (Vialard et al., 2025; Vijayeta & Dommenges, 2018; Wengel et al., 2018).

We similarly fit the NRO parameters using Equations 5 and 6 as in Vialard et al. (2025). We perform linear regression of the monthly mean tendencies of T on T , h , T^2 , T^3 to obtain estimates for the parameters R , F_1 , b , and c . Estimates for ϵ and F_2 are obtained using the same fit described above, since Equations 2 and 6 are identical.

Given estimates for R , ϵ , F_1 , and F_2 obtained by fitting either the LRO or the NRO, we estimate the growth rate and period using the BWJ index (Equations 3 and 4, Jin et al., 2006, 2020; Lu et al., 2018).

3. Results

We now describe the results regarding the accuracy of estimating the RO parameters from simulated time series, where we know the true model parameter values used to generate the time series. We then consider the implications for our ability to distinguish between a damped and a self-sustained oscillation in the presence of noise as pertains to ENSO in the climate system.

We first reiterate the known result (Burgers et al., 2005; Jin, 1997a) that both a damped and a self-sustained RO can match the characteristics of ENSO found in observations (Figure 1). We analyze simulated time series of the mean monthly anomalies, T and h , for a damped system with a decay timescale of 1.7 years (Figure 1a) and for a self-sustained system with a growth timescale of 11 years (Figure 1b). We compare the distributions of the simulated monthly values for T to those from observations and find similar centers and spread among the three distributions (Figure 1c). Han et al. (2025) recently found that self-sustained RO simulations often lead to bimodal distributions of T , but we find that appropriate levels of noise yield reasonable distributions of T . However, we note that neither simulated system reproduces the extreme events found in the observed time series (T around 2.5 K and greater); identifying the minimal RO model that produces extreme events remains an area of open research, and may involve multiplicative, SST-dependent stochastic forcing representing westerly wind bursts (e.g., Eisenman et al., 2005; Tziperman & Yu, 2007; Vialard et al., 2025). We also compute the spectrum of the simulated and observed time series for T and find strong agreement (Figure 1d). All three spectra show a peak corresponding to an average period of around 3.7 years, consistent with an ENSO period of approximately 2–5 years (Jiang et al., 2021).

Next, we estimate the RO parameters R , ϵ , F_1 , and F_2 by fitting the LRO Equations 1 and 2 to our simulated time series for T and h and compute the estimated growth rate and period (3, 4). The distributions of the estimated growth rate and period across 100 simulations for both the damped and self-sustained systems are shown in Figures 1e and 1f. We find that, for the damped system, the fit tends to estimate weaker damping than the true value and, for the self-sustained system (positive growth rate), the fit consistently estimates a damped system (negative estimated growth rate) across all simulations (Figure 1e). The estimates of the period are more accurate, with most estimates falling within 6 months of the true simulated period (Figure 1f). These results suggest that fitting the linear RO to data may not be able to accurately estimate the growth rate and may estimate a damped system (negative growth rate) when the system is self-sustained (positive growth rate).

To see which LRO parameters are not well estimated by the fit, Figure 2 shows distributions of the estimates for the four linear model parameter values across 100 simulated time series compared to their true value. For both the damped and self-sustained cases, the true value of ϵ , F_1 , and F_2 fall within the range of estimated values (Figures 2b–2d). However, for all parameters, we note that the mean estimate over many simulations does not appear to match the true value. The estimates for R show large errors, particularly for the self-sustained system, where the estimates of R have the incorrect sign for all simulations (Figure 2a). The growth rate depends on R and ϵ (Equation 3), so these large errors in the estimates for R translate into the large errors in the estimates of the growth rate (Figure 1e). In particular, for the self-sustained case, the large negative estimated value for R when the true value is positive results in the estimated growth rate suggesting a damped system despite the simulated system being self-sustained. The period depends on all four parameters, with the product $F_1 F_2$ being the dominant

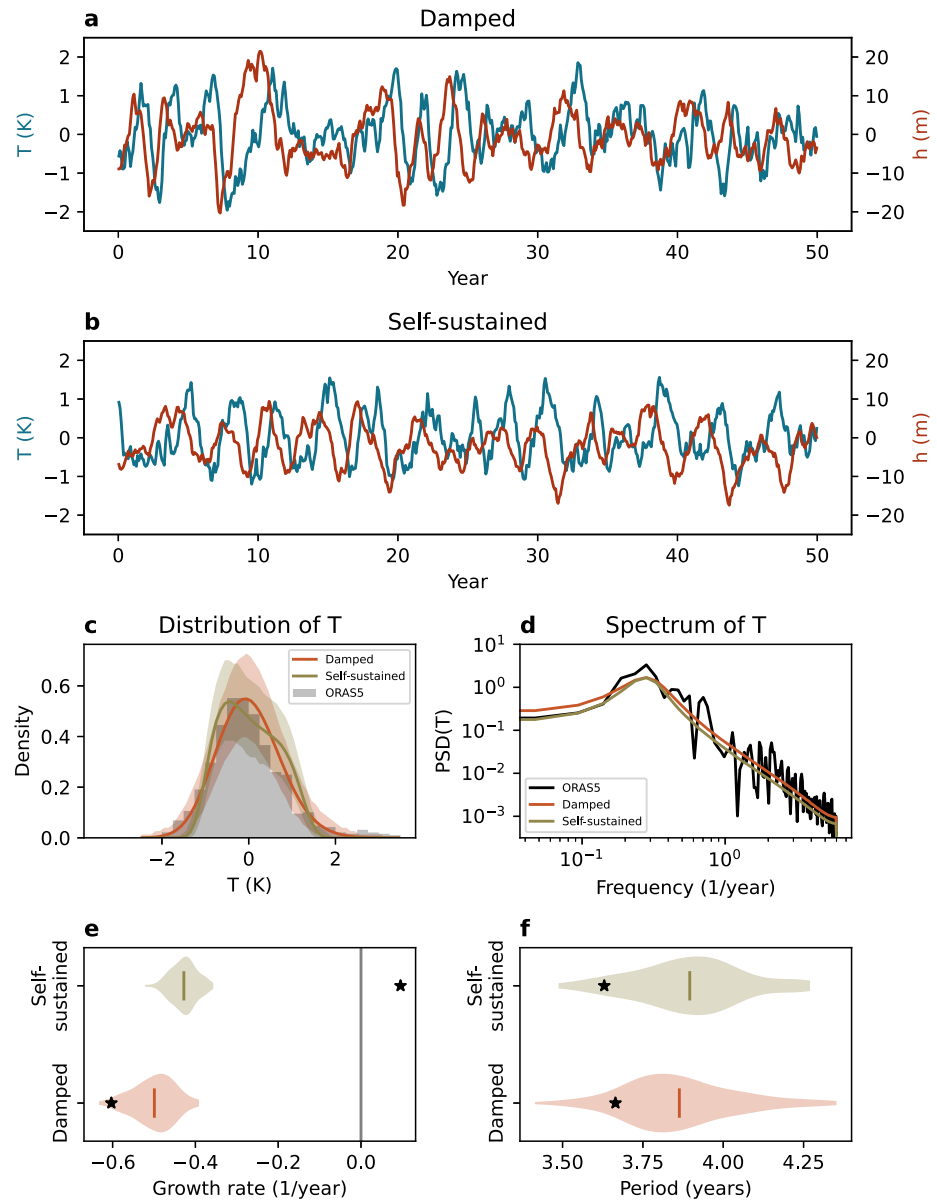


Figure 1. Comparison between a simulated damped recharge oscillator, a simulated self-sustained recharge oscillator, and observations. (a) Time series of T (blue) and h (red) for a damped system. (b) Time series of T (blue) and h (red) for a self-sustained system. (c) Comparison of the distributions of T for observations and simulated damped and self-sustained cases. For the simulated cases, the solid lines indicate the distribution generated from a 10,000-year time series. The shaded regions indicate the possible range in the simulated distributions when the time series is subsampled to match the length of the observations. (d) Comparison of the spectra of T for observations and simulated damped and self-sustained cases. Estimates of the growth rate (e) and period (f) obtained by fitting the LRO to the simulated time series. The stars indicate the true parameter values used to produce the simulated time series.

term under the radical in Equation 4. Therefore, the period is less sensitive to the errors in estimates for R , and estimates of the period tend to be closer to the true value due to the smaller errors in the estimates of F_1 and F_2 .

Fitting the LRO using a longer time series reduces the variance in the estimates, but the error in the mean of the estimates persists (Figure S1 in Supporting Information S1) implying that the errors in the mean estimates seen in Figures 1e and 1f are not due to sampling issues. Instead, these results suggest that fitting the LRO to the time series may lead to a biased estimate for the parameters of interest, that is, the mean of the parameter estimates does not approach the true value even when more simulations are performed or when longer time series are used. The

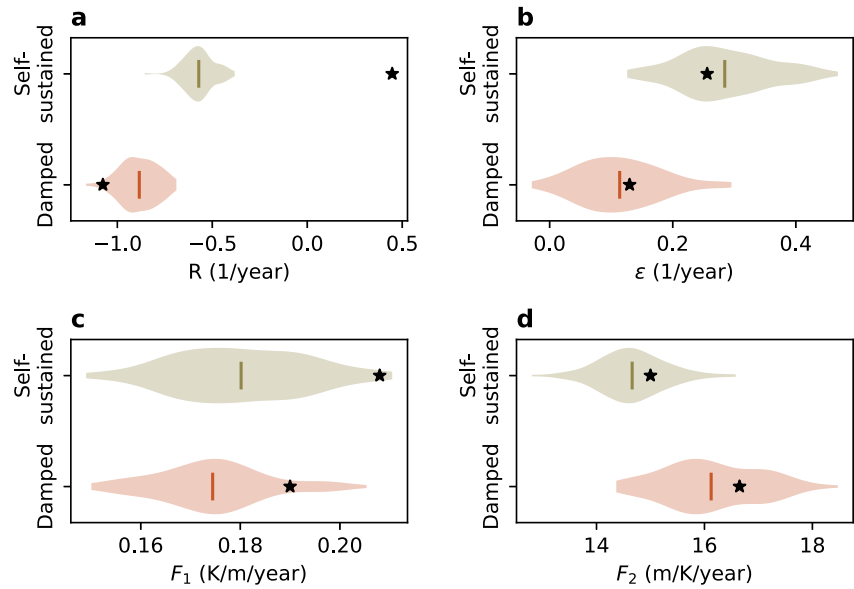


Figure 2. Estimates of the RO parameters—(a) R , (b) ϵ , (c) F_1 , (d) F_2 —obtained by fitting the LRO to the simulated time series. Stars indicate the true parameter values.

bias in this estimator may have several possible explanations, including mismatch between the models used to produce and fit the data (which is an expected difficulty when fitting the LRO to GCMs or observations), averaging over nonlinearities in the model, and serial autocorrelation in the noise terms (Section 3.3.3, James et al., 2013).

To diagnose the source of the bias, we perform a series of experiments in which we modify the method used to estimate the RO parameters in a number of ways including fitting the NRO (instead of the LRO) equations, using daily (instead of monthly) data to fit the RO equations, and fitting simulations produced using white (instead of red) noise. Ultimately, we find that fitting the NRO equations using monthly data reduces the bias, fitting daily data can actually increase the bias, and only fitting daily data that was simulated using white noise allows us to achieve unbiased estimates. These results lead us to conclude that there are two primary sources of bias—first, the omission of correlated model variables that occurs when fitting the LRO to simulations produced by the NRO and, second, the correlation between the noise terms and model variables; these violate the strict exogeneity condition, which states that explanatory variables (T and h in our case) are not correlated with the error term in a regression model. This condition is required for ordinary least squares to be an unbiased estimator. We discuss these results and conclusions further below.

The errors in the estimates of the growth rate and period are smaller when the NRO equations are fit to monthly data (Figures S3a and S3b in Supporting Information S1) compared to when the LRO equations are fit to monthly data (Figures 1e and 1f). The reduction in the error is especially notable for the self-sustained case, where the magnitude of the nonlinear coefficients are larger. This result suggests that, when the LRO equations are fit to data simulated using the NRO, the omission of the quadratic and cubic nonlinearities in the fit model leads to omitted variable bias (Section 13.3, Wasserman, 2004) due to the correlation between the omitted variables (T^2 and T^3) with the included variables.

Fitting the NRO equations using daily data instead of monthly seems to improve our estimates of the growth rate in the self-sustained case, but actually leads to larger errors of the growth rate in the damped case (Figures S3a and S3c in Supporting Information S1). While one might expect that using more frequent data to perform the fit and compute parameter estimates should reduce the errors due to a reduced averaging over the nonlinearity, these results suggest a different source of bias. The larger bias in this case is likely due to the correlation between the noise terms and the regressor variables (T and h). The autocorrelation in the simulated noise term, combined with the serial time dependence of T and h , leads to a correlation between the noise terms and the model variables, which violates the strict exogeneity assumption required for ordinary least squares to be an unbiased estimator

(Section 13.3, Wasserman, 2004). For a linear model of the form $y = X\beta + \epsilon$, the bias in the estimated coefficients (estimates of β) is given by $(X^T X)^{-1} X^T \epsilon$. If $E[\epsilon|X] = 0$ (i.e., the expected value (average) of the error term ϵ , given any value of the regressor variable(s) X is zero; this is the strict exogeneity condition), then the estimates of the coefficients will be unbiased. However, correlation between the noise term ϵ and the model variables X leads to a nonzero bias term. In the experiments described here, this correlation is more pronounced in the daily data than the monthly data due to the relative lengths of the autocorrelation and averaging timescales. The noise was simulated with a decorrelation timescale of 3 days, so averaging over the longer (monthly) timescale effectively whiten the character of the noise and weakens the correlation of the noise with the model variables T and h . The magnitude and sign of the bias term depends on many factors, including the character of the noise and the true values of the coefficients on the nonlinear terms, b and c .

Finally, we find that we achieve unbiased estimates of the growth rate and period when we estimate the RO parameters by fitting the NRO equations to daily data simulated using white noise (Figures S3e and S3f in Supporting Information S1). Simulating the time series with white noise forcing that has no autocorrelation structure effectively eliminates the correlation between the noise terms and the model variables such that the strict exogeneity condition is now satisfied. Only under these conditions—including no mismatch between the dynamics producing the data and those of the fitted model, high temporal resolution data, and uncorrelated noise forcing used in the simulation—do we find this method of estimating the RO parameters to return unbiased estimates. We note that fitting the LRO equations to daily data simulated using white noise for the damped case also seems to produce unbiased estimates of the growth rate and period (Figures S2c and S2d in Supporting Information S1). This result suggests that for the damped case where the nonlinear effects are weak, it is the correlation between the noise terms and model variables that dominates the source of the bias in Figures 1e and 1f. In general, we also find that improved estimates of the growth rate and period coincide with improved estimates of the coefficients on the nonlinear terms (Figure S4 in Supporting Information S1).

Ultimately, we cannot expect to satisfactorily address all of these sources of bias when fitting the RO to observations. First, we do not know the exact dynamics for ENSO in the climate system. The RO is a very useful conceptual model but is not meant to capture the full complexity of ENSO, so we can always expect some mismatch between the model's dynamics and those that govern the observed system. Additionally, the true structure of the noise and its relationship to ENSO variables in the climate system is unknown. The noise term in the RO model is typically considered to represent weather noise and westerly wind bursts, whose correlation time is on the order of a week and whose magnitude and direction may also depend on the ENSO state. These characteristics of the noise in the climate system mean that the strict exogeneity condition required for unbiased ordinary least squares parameter estimates is likely to be violated in observations of ENSO. Given these constraints, we expect it would be difficult to correctly diagnose whether the observed ENSO is damped or self-sustained using the analysis tools examined here.

Up to this point, we have considered two sets of representative parameter values corresponding to a self-sustained and a damped regime. We do not know the RO parameter values that would most accurately describe the observed ENSO. We now consider a broad range of RO parameter values for R , ϵ , F_1 , F_2 , b , c , $\text{std}(\zeta_T)$, and $\text{std}(\zeta_H)$, producing corresponding time series for each set of parameters. We simulated 10,000 such time series for T and h in which the model period ranges from 0 to 10 years, and the growth rate ranges from -1 to 1 year^{-1} . We randomly generated values for all NRO parameters producing ENSO time series with growth rates between -1 and 1 years^{-1} and periods between 1 and 10 years, allowing for any combination of these. We then followed the same method as above for estimating R , ϵ , F_1 , and F_2 by fitting the LRO equations to the monthly mean anomalies.

Figures 3a–3d show the comparison between the true and estimated parameter values, growth rate, and period. We find that this fit of the RO parameters underestimates the true growth rate and overestimates the true period on average (Figures 3a and 3b). Most strikingly, when the true growth rate is positive, the estimated growth rate is effectively always negative (Figure 3a). This means that when the true system is self-sustained, this approach will likely lead to the incorrect conclusion that the system is damped. We note that while the growth rate is underestimated on average, it remains possible to overestimate the growth rate for certain parameter regimes such as for the damped case in Figure 1e. While Figure 3 reflects the results across a range of values for b and c , the direction of the bias depends on the correlation structure of the noise and the magnitude of b and c as previously discussed. Nonetheless, the error in the growth rate appears to mainly be due to errors in the estimated value for R

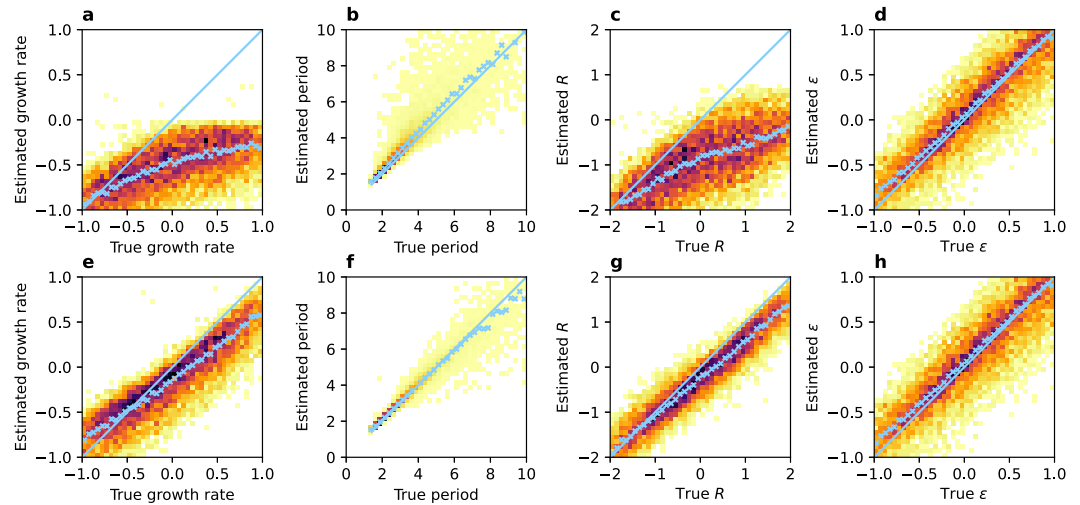


Figure 3. Comparison of estimates of the RO parameters—(a, e) growth rate, (b, f) period, (c, g) R , (d, h) ϵ —obtained by fitting the LRO (a–d) or NRO (e–h) to the simulated time series with the true values. Time series were simulated according to the NRO, varying the true values of R , ϵ , F_1 , F_2 , b , and c . Color shading indicates the number of simulations falling into each pixel (representing a range of true and estimated parameter values). The one-to-one line is shown in blue. \times s indicate binned mean estimates.

(Figure 3c). When the true growth rate is greater than zero, the estimated growth rate is consistently around -0.27 year^{-1} (a decay scale of 4 years). As a reminder, when the LRO is fit to observations, the estimated growth rate is -0.53 year^{-1} . In short, it appears that estimating a negative growth rate by fitting the LRO may incorrectly suggest a damped system, even when the true dynamics are self-sustained.

Having previously shown that fitting the LRO when the model generating the data was nonlinear contributes to the errors we find in estimating the RO parameters, we now repeat our previous analysis but fit the NRO equations to our simulated time series. This analysis allows us to explore the accuracy of our parameter estimates when the model generating the data exactly matches the model that we fit. While the errors are smaller, this fit still tends to underestimate the value of R (Figure 3g) and overestimate the value of ϵ (Figure 3h), both of which contribute to underestimating the growth rate (Figure 3e). The values of b and c tend to be well estimated when their magnitude is small, but the errors in the estimates grow as the magnitude of the nonlinear terms increase (Figure S5 in Supporting Information S1). The larger errors in R are likely accompanied by these errors in high values of b and c . Ultimately, only once the true growth rate is above 0.23 year^{-1} do we estimate a positive growth rate on average. When we fit the NRO to observations, we estimate a growth rate of -0.6 year^{-1} .

When fitting observations, one expects the dynamics to have some differences from the fitted model. We test the sensitivity of the accuracy of the parameter estimates to this by fitting a different nonlinearity than the nonlinearity included in the model generating the data. For this test, we remove the cT^3 term from the equation for the evolution of the SST and simulate the time series with a ch^3 term in the equation for the evolution of the thermocline depth instead. Then, we fit the nonlinear model with the cT^3 term in the equation for the evolution of the SST as described by Equation 5 and 6. We find that fitting the wrong nonlinearity (as is likely to be the case when fitting a simple model to observations or climate model output) can yield errors in estimates of the growth rate as large as those found by fitting the LRO to simulations produced using the NRO (Figure S6 in Supporting Information S1).

These results suggest that the parameter errors found by fitting the correct model represent a lower bound for the errors. The errors when fitting to observations are expected to be even larger, because we cannot expect the RO model to perfectly represent the observed dynamics. Therefore, fitting the RO to observations or climate model output likely underestimates the true ENSO growth rate.

4. Conclusions

We have investigated the potential for characterizing ENSO as a damped or a self-sustained regime by fitting the recharge oscillator (RO) to observations or climate model output via multivariate linear regression. Previous work fitting the RO, both linear and nonlinear, to observations and climate model output have consistently yielded results that suggest ENSO is a damped oscillator. Here, we explore the robustness of this approach. By leveraging simulations of RO time series for which we know the true parameter values, we attempt to quantify the error in the parameter estimates obtained by fitting the RO equations. We then considered how these errors in the RO parameters affect the inferred growth rate and period of ENSO.

We have found that estimating the ENSO growth rate using this fitting approach consistently underestimates the growth rate of ENSO. Not surprisingly, the errors in the estimates are greater when the fitted model is not identical to the model generating the data, as would be the case when fitting observations and climate model output. We found that a damped ENSO is often identified even when the simulated system was self-sustained. Overall, our results suggest that it would be challenging to robustly differentiate between damped and self-sustained ENSO regimes by estimating the growth rate from the fitted RO parameters. This problem is especially severe when the LRO is fit, where the estimated growth rate is effectively never self-sustained over a wide range of parameters explored for the model used to generate the fitted data.

A less damped ENSO regime suggested by our results is consistent with estimates of the ENSO growth rate in Jin et al. (2020) based on analytic formulae for the RO parameters. Their estimates yielded a growth rate of -0.3 year^{-1} (a 3-year decay time scale), which they note implied that the ENSO dynamics are near critical. This estimate represents much weaker damping than typical estimates from fitting the RO parameters via linear regression. For example, we estimated the ENSO growth rate to be -0.53 year^{-1} when fitting the LRO to observations, (a 1.9 years damping time scale, consistent with Burgers et al. (2005), Wengel et al. (2018), Vijayeta and Dommenget (2018), Vialard et al. (2025)). Jin et al. (2020) attribute the differences to nonlinearities being captured in the linear fitting method but not in their analytic formulae. Our results suggest that the difference could also be due to biased estimation of the growth rate when fitting the RO to observations.

In a recent study aimed at identifying an optimal set of RO parameters, Han et al. (2025) found that the damped case is most likely. Instead of fitting the RO parameters using a regression approach, they performed a parameter sweep to identify the optimal set of RO parameters that reproduce the observed ENSO characteristics such as the standard deviation, skewness, and kurtosis of T . While Han et al. (2025) concluded that the optimal RO parameters correspond to a damped system, we do not find conclusive evidence either way.

Our study is based on input produced by the RO equations to test the fit by the RO, and therefore provides a lower bound for the errors in the parameter estimates. It would be more challenging to estimate the expected errors one would find by fitting the RO to observations or climate model output, as the extent of model mismatch between the RO and observations is unknown. For example, the RO does not explicitly model the Kelvin Wave dynamics involved in the central-to-eastern Pacific thermocline adjustment (Bosc & Delcroix, 2008; McPhaden, 2012; Meinen & McPhaden, 2000), nor does the RO model allow for potential hemispheric asymmetries in the winds or mass transport to be represented (Kug et al., 2003). These simplifications limit the RO's ability to capture these details of the dynamics, and are an example of dynamical mismatches that may result in additional challenges in distinguishing between the damped and self-sustained regimes. Additionally, we followed previous studies and fitted both linear and nonlinear RO models, yet other variations on the NRO exist, such as models that include a multiplicative noise term or allow the value of F_1 to depend on the sign of h . Fitting other variants of the RO may yield different estimates for the error lower bound.

In summary, our results show that the ENSO growth rate is likely underestimated by fitting the RO to observations or climate model output. This underestimation can yield a negative estimated growth rate (damped oscillatory regime) even when the dynamics are characterized by a positive growth rate (self-sustained regime). The challenges in distinguishing between a damped and a slightly supercritical system were clearly noted by Burgers et al. (2005). Similarly, it is well-known that a self-sustained chaotic description of ENSO is difficult to distinguish from a damped oscillatory stochastically driven regime, although with a long enough time series there are tools that allow one to distinguish between the two (Tziperman et al., 1994). We also note the possibility of a third regime in which the damping is so strong that the decay timescale is significantly shorter than the typical time between events. In this case, subsequent ENSO events are effectively independent of each other, and the

system could be more accurately characterized as a series of events rather than an oscillatory cycle (Kessler, 2002). However, given the magnitude of the errors likely to occur in estimating the decay rate, it would be similarly challenging to isolate this regime using the approaches discussed here. Our results ultimately highlight the potential challenges of a specific method that has been used to estimate ENSO's growth rate and show that it may therefore not be straightforward to determine whether ENSO is a damped or self-sustained oscillator.

Data Availability Statement

The ORAS5 reanalysis data used for this paper is available at Copernicus Climate Change Service (2021). Numerical simulations and python code used to generate the results and figures in this work can be found at Zenodo (Weeks, 2025).

Acknowledgments

This work was funded by Department of Energy (DOE) Office of Science Biological and Environmental Research Grant DE-SC0023134. ET thanks the Weizmann Institute of Science for its hospitality during parts of this work.

References

- Battisti, D. S., & Hirst, A. C. (1989). Interannual variability in a tropical atmosphere–ocean model: Influence of the basic state, ocean geometry and nonlinearity. *Journal of the Atmospheric Sciences*, *46*(12), 1687–1712. [https://doi.org/10.1175/1520-0469\(1989\)046<1687:iviata>2.0.co;2](https://doi.org/10.1175/1520-0469(1989)046<1687:iviata>2.0.co;2)
- Bosc, C., & Delcroix, T. (2008). Observed equatorial Rossby waves and ENSO-related warm water volume changes in the equatorial Pacific Ocean. *Journal of Geophysical Research*, *113*(C6). <https://doi.org/10.1029/2007jc004613>
- Burgers, G., Jin, F.-F., & Van Oldenborgh, G. J. (2005). The simplest ENSO recharge oscillator. *Geophysical Research Letters*, *32*(13). <https://doi.org/10.1029/2005gl022951>
- Capotondi, A., Wittenberg, A. T., Kug, J.-S., Takahashi, K., & McPhaden, M. J. (2020). ENSO diversity. In *El Niño southern Oscillation in a changing climate* (pp. 65–86).
- Chang, P., Ji, L., Li, H., & Flügel, M. (1996). Chaotic dynamics versus stochastic processes in El Niño–Southern Oscillation in coupled ocean–atmosphere models. *Physica D: Nonlinear Phenomena*, *98*(2–4), 301–320. [https://doi.org/10.1016/0167-2789\(96\)00116-9](https://doi.org/10.1016/0167-2789(96)00116-9)
- Chen, C., Cane, M. A., Wittenberg, A. T., & Chen, D. (2017). ENSO in the CMIP5 simulations: Life cycles, diversity, and responses to climate change. *Journal of Climate*, *30*(2), 775–801. <https://doi.org/10.1175/jcli-d-15-0901.1>
- Copernicus Climate Change Service, C. D. S. (2021). ORAS5 global ocean reanalysis monthly data from 1958 to present [Dataset]. *Copernicus Climate Change Service (C3S) Climate Data Store (CDS)*. <https://doi.org/10.24381/cds.67e8eeb7>
- Eisenman, I., Yu, L. S., & Tziperman, E. (2005). Westerly wind bursts: ENSO's tail rather than the dog? *Journal of Climate*, *18*(24), 5224–5238. <https://doi.org/10.1175/JCLI3588.1>
- Frauen, C., & Dommengat, D. (2010). El Niño and La Niña amplitude asymmetry caused by atmospheric feedbacks. *Geophysical Research Letters*, *37*(18). <https://doi.org/10.1029/2010GL044444>
- Frauen, C., & Dommengat, D. (2012). Influences of the tropical Indian and Atlantic Oceans on the predictability of ENSO. *Geophysical Research Letters*, *39*(2). <https://doi.org/10.1029/2011gl050520>
- Guilyardi, E., Capotondi, A., Lengaigne, M., Thual, S., & Wittenberg, A. T. (2020). ENSO modeling: History, progress, and challenges. In *El Niño Southern Oscillation in a changing climate* (pp. 199–226).
- Han, S., Fedorov, A., & Vialard, J. (2025). Realistic ENSO dynamics requires a damped nonlinear recharge oscillator. Retrieved from <https://arxiv.org/abs/2506.11206>
- Harrison, D. E., & Vecchi, G. A. (1997). Westerly wind events in the tropical Pacific, 1986–95. *Journal of Climate*, *10*(12), 3131–3156. [https://doi.org/10.1175/1520-0442\(1997\)010<3131:wweitt>2.0.co;2](https://doi.org/10.1175/1520-0442(1997)010<3131:wweitt>2.0.co;2)
- James, G., Witten, D., Hastie, T., & Tibshirani, R. (2013). *An introduction to statistical learning* (Vol. 112). Springer.
- Jansen, M. F., Dommengat, D., & Keenlyside, N. (2009). Tropical atmosphere–ocean interactions in a conceptual framework. *Journal of Climate*, *22*(3), 550–567. <https://doi.org/10.1175/2008jcli2243.1>
- Jiang, F., Zhang, W., Jin, F.-F., Stuecker, M. F., & Allan, R. (2021). El Niño pacing orchestrates inter-basin Pacific–Indian Ocean interannual connections. *Geophysical Research Letters*, *48*(19), e2021GL095242. <https://doi.org/10.1029/2021gl095242>
- Jin, F.-F. (1997a). An equatorial ocean recharge paradigm for ENSO. Part I: Conceptual model. *Journal of the Atmospheric Sciences*, *54*(7), 811–829. [https://doi.org/10.1175/1520-0469\(1997\)054<0811:aeorpf>2.0.co;2](https://doi.org/10.1175/1520-0469(1997)054<0811:aeorpf>2.0.co;2)
- Jin, F.-F. (1997b). An equatorial ocean recharge paradigm for ENSO. Part II: A stripped-down coupled model. *Journal of the Atmospheric Sciences*, *54*(7), 830–847. [https://doi.org/10.1175/1520-0469\(1997\)054<0830:aeorpf>2.0.co;2](https://doi.org/10.1175/1520-0469(1997)054<0830:aeorpf>2.0.co;2)
- Jin, F.-F., Chen, H.-C., Zhao, S., Hayashi, M., Karamperidou, C., Stuecker, M. F., et al. (2020). Simple ENSO models. In *El Niño Southern Oscillation in a changing climate* (pp. 119–151).
- Jin, F.-F., Kim, S. T., & Bejarano, L. (2006). A coupled-stability index for ENSO. *Geophysical Research Letters*, *33*(23). <https://doi.org/10.1029/2006gl027221>
- Jin, F.-F., Lin, L., Timmermann, A., & Zhao, J. (2007). Ensemble-mean dynamics of the ENSO recharge oscillator under state-dependent stochastic forcing. *Geophysical Research Letters*, *34*(3). <https://doi.org/10.1029/2006gl027372>
- Kessler, W. S. (2002). Is ENSO a cycle or a series of events? *Geophysical Research Letters*, *29*(23), 40–41. <https://doi.org/10.1029/2002gl015924>
- Kim, S. T., Cai, W., Jin, F.-F., & Yu, J.-Y. (2014). ENSO stability in coupled climate models and its association with mean state. *Climate Dynamics*, *42*(11–12), 3313–3321. <https://doi.org/10.1007/s00382-013-1833-6>
- Kim, S. T., & Jin, F.-F. (2011). An ENSO stability analysis. Part II: Results from the twentieth and twenty-first century simulations of the CMIP3 models. *Climate Dynamics*, *36*(7–8), 1609–1627. <https://doi.org/10.1007/s00382-010-0872-5>
- Kug, J.-S., Kang, I.-S., & An, S.-I. (2003). Symmetric and antisymmetric mass exchanges between the equatorial and off-equatorial Pacific associated with ENSO. *Journal of Geophysical Research*, *108*(C8). <https://doi.org/10.1029/2002jc001671>
- Latif, M., Sperber, K., Arblaster, J., Braconnot, P., Chen, D., Colman, A., et al. (2001). ENSIP: The El Niño simulation intercomparison project. *Climate Dynamics*, *18*(3–4), 255–276. <https://doi.org/10.1007/s003820100174>
- Levine, A. F., & McPhaden, M. J. (2015). The annual cycle in ENSO growth rate as a cause of the spring predictability barrier. *Geophysical Research Letters*, *42*(12), 5034–5041. <https://doi.org/10.1002/2015gl064309>

- Lu, B., Jin, F.-F., & Ren, H.-L. (2018). A coupled dynamic index for ENSO periodicity. *Journal of Climate*, 31(6), 2361–2376. <https://doi.org/10.1175/jcli-d-17-0466.1>
- Maher, N., Wills, R. C. J., DiNezio, P., Klavans, J., Milinski, S., Sanchez, S. C., et al. (2023). The future of the El Niño–Southern Oscillation: Using large ensembles to illuminate time-varying responses and inter-model differences. *Earth System Dynamics*, 14(2), 413–431. <https://doi.org/10.5194/esd-14-413-2023>
- McPhaden, M. J. (2012). A 21st century shift in the relationship between ENSO SST and warm water volume anomalies. *Geophysical Research Letters*, 39(9). <https://doi.org/10.1029/2012gl051826>
- Meinen, C. S., & McPhaden, M. J. (2000). Observations of warm water volume changes in the equatorial Pacific and their relationship to El Niño and La Niña. *Journal of Climate*, 13(20), 3551–3559. [https://doi.org/10.1175/1520-0442\(2000\)013<3551:oowwvc>2.0.co;2](https://doi.org/10.1175/1520-0442(2000)013<3551:oowwvc>2.0.co;2)
- Neelin, J. D., Battisti, D. S., Hirst, A. C., Jin, F.-F., Wakata, Y., Yamagata, T., & Zebiak, S. E. (1998). ENSO theory. *Journal of Geophysical Research*, 103(C7), 14261–14290. <https://doi.org/10.1029/97jc03424>
- Perez, C. L., Moore, A. M., Zavala-Garay, J., & Kleeman, R. (2005). A comparison of the influence of additive and multiplicative stochastic forcing on a coupled model of ENSO. *Journal of Climate*, 18(23), 5066–5085. <https://doi.org/10.1175/jcli3596.1>
- Planton, Y. Y., Guilyardi, E., Wittenberg, A. T., Lee, J., Gleckler, P. J., Bayr, T., et al. (2021). Evaluating climate models with the CLIVAR 2020 ENSO metrics package. *Bulletin of the American Meteorological Society*, 102(2), E193–E217. <https://doi.org/10.1175/bams-d-19-0337.1>
- Schopf, P. S., & Suarez, M. J. (1988). Vacillations in a coupled ocean-atmosphere model. *Journal of the Atmospheric Sciences*, 45(3), 549–566. [https://doi.org/10.1175/1520-0469\(1988\)045<0549:viacom>2.0.co;2](https://doi.org/10.1175/1520-0469(1988)045<0549:viacom>2.0.co;2)
- Suarez, M. J., & Schopf, P. S. (1988). A delayed action oscillator for ENSO. *Journal of the Atmospheric Sciences*, 45(21), 3283–3287. [https://doi.org/10.1175/1520-0469\(1988\)045<3283:adaofe>2.0.co;2](https://doi.org/10.1175/1520-0469(1988)045<3283:adaofe>2.0.co;2)
- Timmermann, A., An, S.-I., Kug, J.-S., Jin, F.-F., Cai, W., Capotondi, A., et al. (2018). El Niño–Southern Oscillation complexity. *Nature*, 559(7715), 535–545. <https://doi.org/10.1038/s41586-018-0252-6>
- Tziperman, E., Cane, M. A., & Zebiak, S. E. (1995). Irregularity and locking to the seasonal cycle in an ENSO prediction model as explained by the quasi-periodicity route to chaos. *Journal of the Atmospheric Sciences*, 52(3), 293–306. [https://doi.org/10.1175/1520-0469\(1995\)052<0293:ialts>2.0.co;2](https://doi.org/10.1175/1520-0469(1995)052<0293:ialts>2.0.co;2)
- Tziperman, E., Stone, L., Cane, M. A., & Jarosh, H. (1994). El Niño chaos: Overlapping of resonances between the seasonal cycle and the Pacific ocean-atmosphere oscillator. *Science*, 264(5155), 72–74. <https://doi.org/10.1126/science.264.5155.72>
- Tziperman, E., & Yu, L. (2007). Quantifying the dependence of westerly wind bursts on the large scale equatorial Pacific SST. *Journal of Climate*, 20(12), 2760–2768. <https://doi.org/10.1175/jcli4138a.1>
- Vallis, G. K. (1986). El Niño: A chaotic dynamical system? *Science*, 232(4747), 243–245. <https://doi.org/10.1126/science.232.4747.243>
- Vecchi, G. A., & Wittenberg, A. T. (2010). El Niño and our future climate: Where do we stand? *Wiley Interdisciplinary Reviews: Climate Change*, 1(2), 260–270. <https://doi.org/10.1002/wcc.33>
- Vialard, J., Jin, F.-F., McPhaden, M. J., Fedorov, A., Cai, W., An, S.-I., et al. (2025). The El Niño southern oscillation (ENSO) recharge oscillator conceptual model: Achievements and future prospects. *Reviews of Geophysics*, 63(1), e2024RG000843. <https://doi.org/10.1029/2024rg000843>
- Vijayeta, A., & Dommenget, D. (2018). An evaluation of ENSO dynamics in CMIP simulations in the framework of the recharge oscillator model. *Climate Dynamics*, 51(5), 1753–1771. <https://doi.org/10.1007/s00382-017-3981-6>
- Wasserman, L. (2004). *All of statistics: A concise course in statistical inference*. Springer Science & Business Media.
- Weeks, E. (2025). Replication data and code for the figures in: “Challenges in determining whether ENSO is a damped or a self-sustained oscillation,” by Elle Weeks and Eli Tziperman, submitted to Geophysical Research Letters. [Collection]. *Zenodo*. <https://doi.org/10.5281/zenodo.15731785>
- Wengel, C., Dommenget, D., Latif, M., Bayr, T., & Vijayeta, A. (2018). What controls ENSO-amplitude diversity in climate models? *Geophysical Research Letters*, 45(4), 1989–1996. <https://doi.org/10.1002/2017gl076849>
- Yu, Y., Dommenget, D., Frauen, C., Wang, G., & Wales, S. (2016). ENSO dynamics and diversity resulting from the recharge oscillator interacting with the slab ocean. *Climate Dynamics*, 46(5–6), 1665–1682. <https://doi.org/10.1007/s00382-015-2667-1>